Anisotropic Ambiguities

Ian F. Jones, Nick X. Bernitsas, Paul A. Farmer, Jennifer M. Leslie, Mike L. Bridson - GX Technology

Abstract

In recent years we have seen a re-writing of many processing algorithms to handle anisotropic effects. For the most part, the type of anisotropy dealt with is VTI or TTI (transverse isotropy, with a vertical or tilted axes) resulting from sedimentary deposition, but azimuthal anisotropy related to sub-vertical fractures is also often considered (HTI).

However, the difficulty in addressing anisotropy lies not in the algorithms, but in reliable estimation of parameters.

In this work, we assess the effects of errors in parameter estimation, and attempt to quantify the consequences of these errors for some specific example.

Introduction

There are three classes of true anisotropy, some with sub-classes:

1. Intrinsic or inherent anisotropy (with 4 sub-classes)
   a) Crystalline anisotropy (with 7 crystal groups)
   b) Constraint induced (e.g. when micro-fissures are held open or closed by lithological confining pressure).
   c) Lithologically induced (e.g. TI due to preferential sedimentary deposition of plate-like grains, or to plate-like crystal formation during metamorphosis)
   d) Paleomagnetically induced (during sedimentation, magnetic minerals will settle with a preferential direction. This may give rise to a detectable seismic anisotropy)
2. Crack induced anisotropy
This type of anisotropy is governed by large scale fractures which readily manifest themselves with a seismic response (this has a different form from the micro fractures which are controlled by confining pressure)
3. Long wavelength anisotropy (with 2 sub-classes)
This is a compound effect created by placing many adjacent regions next together: each region itself may be isotropic, but the net effect creates a form of anisotropy. There are two sub-classes here:
   a) Periodic thin layered
   b) Checkerboard

Due to symmetries, the 81 components of the elastic compliance tensor reduce to 21; we can also have further reductions to this complexity. For the transversely isotropic case, which we deal with in this work, approximations can be made such that only one additional parameter is required to describe the problem for time imaging, and two additional parameters for depth imaging.

The commonest formulations of these parameters are those described by Thomsen (1984), and those described by Alkhalifah & Tsvankin (1995). For time domain data, we can assess the degree of residual curvature on the far traces with the Alkhalifa eta parameter, and for depth imaging, we can describe the depth discrepancy and residual far offset moveout with Thomsen's delta and epsilon parameters (respectively).

The delta parameter is most easily obtained from the mis-match between a well and the depth migrated seismic image, and the epsilon parameter either from far offset residual moveout analysis, or from tomographic inversion.

North Sea Example

The real data shown here comes from an area with a thick anisotropic shale overburden, and targets below the BCU (Base Cretaceous unconformity). In Figure 1, we see a CRP gather resulting from three different runs of 3D preSDM. In the first, we have an isotropic migration, where the velocity model was built so as to flatten the CRP gather. In the second, we have the result from an anisotropic migration with delta estimated from well mis-ties, and with epsilon constrained to equal delta (the elliptical assumption). In the third result, we have estimated epsilon from the far-offset residual moveout (for many shales, epsilon ~ 2delta).

In this case, it is clear that we can improve on isotropic imaging in as much as we tie the well, and preserve the quality of fault imaging after the anelliptic migration. In figure 2, we see the improved fault imaging after anelliptic migration. In addition, a 180m well mis-tie was resolved. These images are converted back to time

Modelling Studies

The question does arise as to whether it is 'safer' to migrate isotropically, and then convert to geological depth (calibrated to the wells) *after* the depth migration. In this case, we would have the trade-off between simplicity in the model building versus potential lateral positioning errors.

An example of this is shown in figure 3. Here we have generated synthetic anisotropic data, and have then migrated it with two different models. The first is the correct model, including anisotropy, used to generate the data. The second was a model derived from the data using tomographic inversion but ignoring the anisotropy. After the migrations, the images have been converted to time with their respective models. In this instance, we see that the error committed by ignoring anisotropy has not significantly degraded the image, nor induced much lateral positioning error.

Conversely, we may have a case where we have ambiguity in the parameter determination due to contributions from other factors which affect the depth and residual far-offset moveout but which may be erroneously interpreted as an anisotropic effect. To assess this problem, we consider examples where a vertical compaction gradient exists in the data, but is incorrectly dealt with in the model building. Some of the travel time effects resulting from the gradient will be then be erroneously accounted for by incorrect determination of anisotropic parameters. For example, preSTM in an isotropic 1D medium using a straight-ray approximation, will give rise to an apparent anisotropy with spurious eta values of about 20%

Alternatively (but not addressed here), as the axis of symmetry for transverse isotropy changes, it becomes difficult to distinguish between TTI and HTI.

We will consider the various possibilities for committing these types of error, and assess the magnitude of these errors.

Conclusions

Including the effects of anisotropy can result in sharper images that correctly tie the wells.

However, including anisotropic effects in the migration can involve error prone estimation of additional parameters.

The nature and magnitude of the error in estimating these parameters will be assessed. Also, the ambiguity in having an error in one parameter, on the determination of another, will be addressed.

References

Alkhalifah, T., & Tsvankin, I., 1995, Velocity analysis for transversely isotropic media; Geophysics, 60, no.5, p1550-1566.
Tatham, R.H., & McCormack, M.D, 1993 - Multicomponent seismology in petroleum exploration; Investigations in Geophysics Series, v6, SEG.
Thomsen,L, 1986, Weal elastic anisotropy; Geophysics, 51, no.10, 1954-1966.

Acknowledgements

The authors wish to thank the TFE UK and CNR UK for kind permission to use their data.

Fig.1: Anisotropic 3D preSDM CRP velocity analysis
(converted to time)

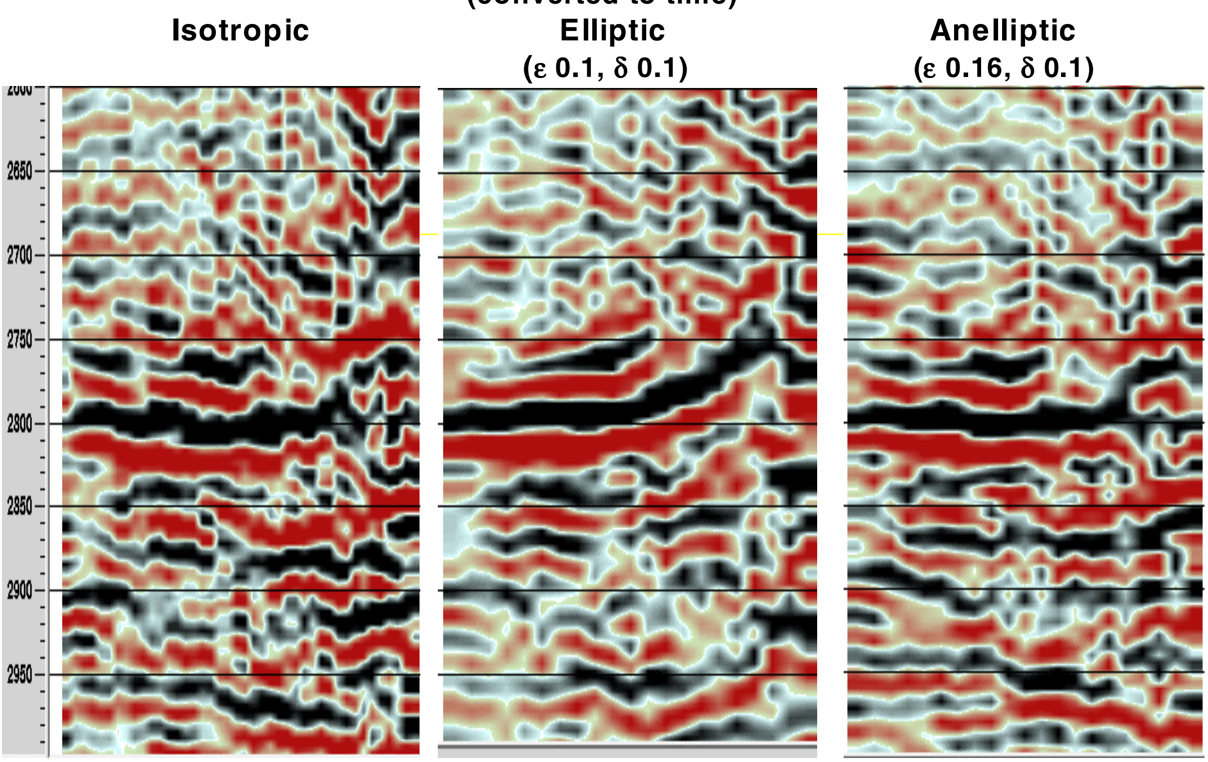

Figure 2.

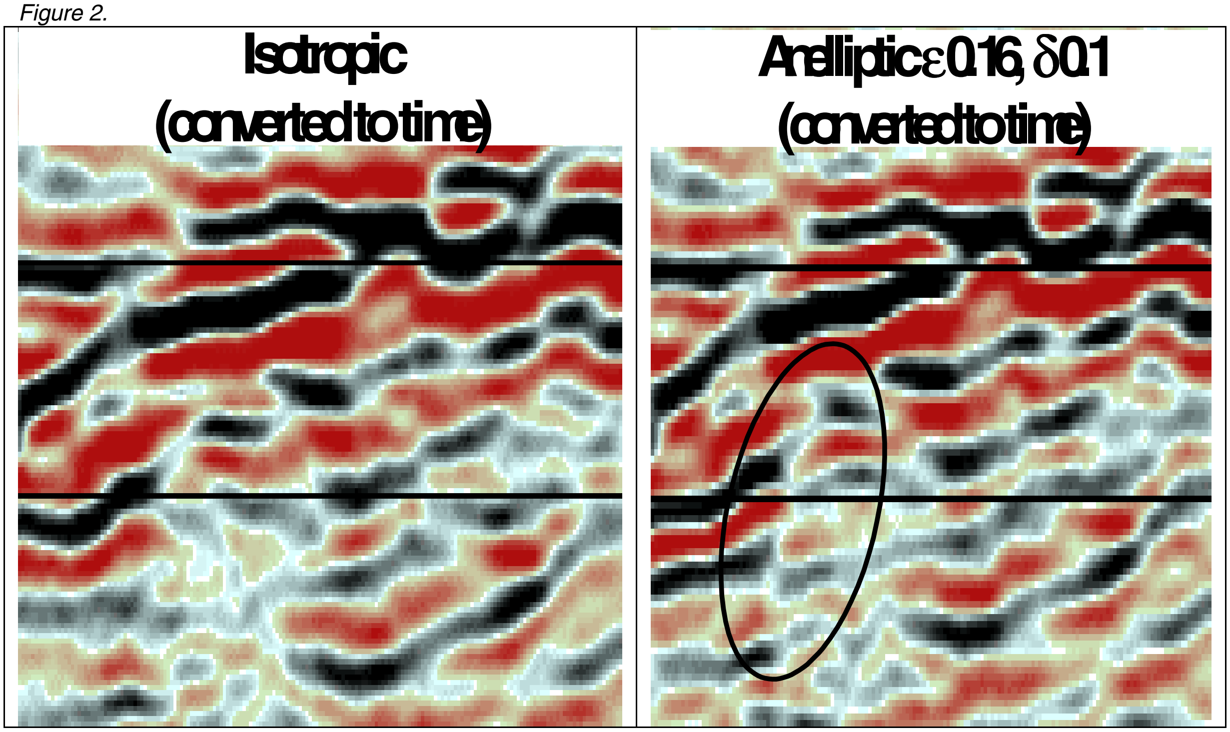

Figure 3.

***Anisotropic** pre-stack depth migration of anisotropic data converted to time*

The migration was run using the model used to create the data

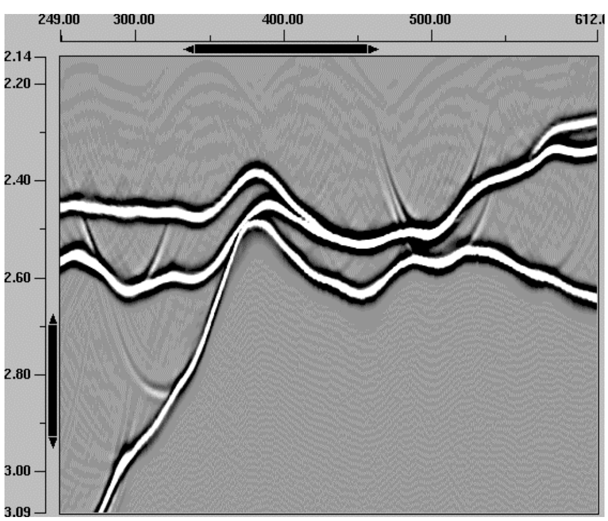

***Isotropic** pre-stack depth migration of anisotropic data converted to time.*

The migration was run using a tomographically derived velocity, but ignoring anisotropy